IIE Transactions

ISSN: 0740-817X (Print) 1545-8830 (Online) Journal homepage: https://www.tandfonline.com/loi/uiie20

Quantitative characterization and modeling strategy of nanoparticle dispersion in polymer composites

Chia-Jung Chang , Lijuan Xu , Qiang Huang & Jianjun Shi

To cite this article: Chia-Jung Chang , Lijuan Xu , Qiang Huang & Jianjun Shi (2012) Quantitative characterization and modeling strategy of nanoparticle dispersion in polymer composites, IIE Transactions, 44:7, 523-533, DOI: 10.1080/0740817X.2011.588995

To link to this article: https://doi.org/10.1080/0740817X.2011.588995

Accepted author version posted online: 17 Jun 2011.
Published online: 23 Apr 2012.

IIE Transactions (2012) **44**, 523–533

ISSN: 0740-817X print / 1545-8830 online
DOI: 10.1080/0740817X.2011.588995

Quantitative characterization and modeling strategy of nanoparticle dispersion in polymer composites

CHIA-JUNG CHANG[1], LIJUAN XU[2], QIANG HUANG[2] and JIANJUN SHI[1,*]

[1] *H. Milton Stewart School of Industrial and Systems Engineering, Georgia Institute of Technology, 765 Ferst Drive, NW, Atlanta, GA 30332, USA*
E-mail: jianjun.shi@isye.gatech.edu
[2] *Daniel J. Epstein Department of Industrial and Systems Engineering, University of Southern California, Los Angeles, CA 90089, USA*

Received June 2010 and accepted March 2011

Nanoparticle dispersion plays a crucial role in the mechanical properties of polymer nanocomposites. Transmission Electron Microscope/Scanning Electron Microscope (TEM/SEM) images are commonly used to represent nanoparticle dispersion without further quantifications on its properties. Therefore, there is a strong need to develop a quantitative measure to effectively describe nanoparticle dispersion from a TEM/SEM image. This article reports an effective modeling strategy to characterize nanoparticle dispersion states among different locations of a nanocomposite surface. An engineering-driven inhomogenous Poisson random field is proposed to represent the nanoparticle dispersion at the nanoscale. The model parameters are estimated through the Bayesian Markov Chain Monte Carlo technique to overcome the challenge of the limited amount of accessible data due to the time-consuming sample collection process. The TEM images taken from nano-silica/epoxy composites are used to support the proposed methodology. The research strategy and framework are generally applicable to other nanocomposite materials.

Keywords: Nanoparticle dispersion, inhomogeneous Poisson random field, Bayesian hierarchical modeling

1. Introduction

Recently, polymer–nanoparticle composite materials have attracted increasing attention due to their unique mechanical, electrical, optical, and thermal properties (Chapman and Mulvaney, 2001; Krishnamoorti and Vaia, 2002; Wilson *et al.*, 2002; Yoon *et al.*, 2002). These unique properties are induced by the properties of the added filler particles and by their interactions with polymer matrices (Balazs *et al.*, 2006; Mackay *et al.*, 2006). Compared to microparticles, nanoparticles have much larger surface areas that facilitate stress transfer from the polymer matrix to the nanoparticles. In addition, the required loadings of nanoparticles in a polymer matrix are usually much lower than those of micro-fillers (Zhang *et al.*, 2006). As a result, when the sizes of filler particles are reduced to nanometer size, dramatic improvements in material properties can be achieved (Kojima *et al.*, 1993; Usuki *et al.*, 1993). Figure 1 shows a Transmission Electron Microscope (TEM) image of a polymer–nanosilica composite and summarizes the improved tensile modulus (the left *y*-axis in Fig. 1(b)) and tensile strength (the right *y*-axis in Fig. 1(b)) of polymer–nanosilica with the volume fraction of nano-SiO_2 introduced (Zhang *et al.*, 2006).

The ultimate material properties of polymer–nanoparticle composites are strongly influenced by their structure, in particular, the states of the nanoparticle dispersion. Experimentally, significantly improved properties are usually observed for a structure possessing a uniform dispersion of nanoparticles in the polymer matrix (Zeng *et al.*, 2008). Taking mechanical properties as an example, a higher degree of filler dispersion has been found to provide a higher composite modulus. In addition to the (i) nature of the polymer–nanoparticle components (e.g., nanofiller, polymer and surfactant); (ii) interactions between the components; and (iii) volume fraction of nanofillers (as illustrated in Fig. 1(b)), the polymer–nanoparticle fabrication process is an influential determinant of nanoparticle dispersion states (Zeng *et al.*, 2008).

The fabrication process for polymer–nanoparticle composites normally starts with a sol-gel process and is followed by mechanical mixing. The sol-gel process is a chemical solution deposition technique in which the material fabrication starts either from a chemical solution (sol) or from colloidal particles to produce an integrated network (gel) (Hench and West, 1990). The sol-gel process has several advantages, including the ability to regulate the proportion

*Corresponding author

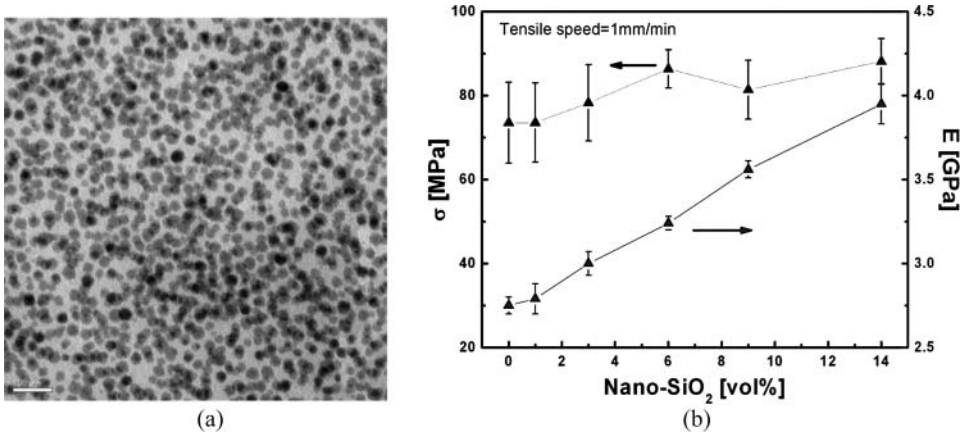

Fig. 1. (a) TEM image of a 14 vol.% silica/epoxy nanocomposite with an average diameter of 25 nm for the nanosilica and (b) the tensile modulus and tensile strength of the SiO_2/epoxy nanocomposites (after Zhang *et al.* (2006)).

of organic and inorganic materials and the monodispersity of the material components (Matejka *et al.*, 1998; Weng *et al.*, 2004). However, the disadvantage posed by this process is its relatively small yield of nanocomposites with only modest mechanical properties. Larger quantities of nanocomposites with superior properties are obtained by mechanically mixing and diluting a master batch of epoxy nanocomposites produced from the sol-gel process with various nanoparticles. The mechanical mixing process significantly extends the limited varieties of nanocomposites offered by the sol-gel processing technique. At the same time, processing conditions during mechanical mixing also have a strong influence on the states of the nanoparticle dispersion and ultimately affect material properties (Mackay *et al.*, 2006).

In spite of the important interdependence between mixing and dispersion, the underlying mechanisms by which mechanical mixing affects particle dispersion have not yet been fully understood. Particle agglomerates, which cause irregular dispersion, defects, and property degradation, often form in nanocomposites and become increasingly problematic when the filler particle content increases (Maskara and Smith, 1997; Zhang *et al.*, 2006). Furthermore, there is currently no quantitative scheme that is able to describe nanoparticle dispersion. Visual judgment of nanocomposite images taken using Scanning Electron Microscope (SEM), TEM or Atomic Force Microscope (AFM) is the only method currently available. Consequently, the development of uniformly dispersed nanocomposites is still largely empirical and a finer degree of control of their properties has to date remained elusive (Zeng *et al.*, 2008). Therefore, in order to achieve nanocomposites with desired mechanical and physical characteristics, the first step should be to quantitatively model and characterize nanoparticle dispersion at the nanoscale. The modeling and characterization will be discussed in further detail throughout the course of this article.

In this article, we propose a hierarchical modeling structure capable of integrating both existing and forthcoming physical understanding to model the dispersion of nanoparticles in the polymer–nanoparticle composite. Through modeling and estimation, we will address the following key issues: (i) how to quantitatively describe the dispersion of nanoparticles in polymer–nanoparticle composites; (ii) how to measure the dispersion of the nanoparticles; and (iii) how to integrate the proposed modeling structure with existing and forthcoming understanding of process–structure–property relations. The objective is to provide a quantitative measure for nanoparticle dispersion and link the dispersion with process and structure characteristics.

This article is organized as follows. Section 2 discusses the modeling of nanoparticle dispersion using an inhomogeneous Poisson random field approach together with the strategies and reasoning for choosing such a modeling approach. Section 3 introduces the Bayesian hierarchical modeling framework proposed for the parameter estimation. Section 4 presents case studies for both simulated data and real collected data to validate and demonstrate our proposed modeling technique. Finally, Section 5 gives a summary of the proposed work and discusses future work.

2. Hierarchical modeling of nanoparticle dispersion at the nanoscale

Let $\mathbf{s}$ be the collection of sites that are regular divisions at the nanoscale of the polymer–nanoparticle composite surface/volume and index them as $1, 2, \ldots, n$. Denote the number of nanoparticles in each site s as $Y(s)$, $s \in \mathbf{s}$. The collection of numbers of nanoparticles at sites $\mathbf{s} = \{1, 2, \ldots, n\}$ is then represented as

$$\mathbf{Y(s)} = \{Y(1), Y(2), \ldots, Y(n)\}^{\mathrm{T}}. \tag{1}$$

What we propose is to model $\mathbf{Y(s)}$ as an inhomogeneous Poisson random field to develop a description of nanoparticle dispersion.

2.1. *Strategy of nanoparticle dispersion modeling*

Due to the lack of physical knowledge and measurement data, Huang (2011) proposed the adoption of a hierarchical modeling strategy for nanomanufacturing process modeling. The effectiveness of hierarchical modeling has been demonstrated in nanowire growth processes (Huang, 2011; Huang *et al.*, 2011). The proposed hierarchical strategy for nanoparticle dispersion modeling includes the following steps.

1. Modeling $\mathbf{Y(s)}$, the collection of numbers of nanoparticles at sites $\mathbf{s} = \{1, 2, \ldots, n\}$ as an inhomogeneous Poisson random field with site dependent intensity function $\lambda(\mathbf{s}, \boldsymbol{\beta})$ where $\boldsymbol{\beta}$ represents the unknown parameters to be specified.
2. Taking into account both process variables, nanoparticle characteristics and nanoparticle interactions for modeling the intensity function $\lambda(\mathbf{s}, \boldsymbol{\beta})$.
3. Taking the intensity function $\lambda(\mathbf{s}, \boldsymbol{\beta})$ as a measure for nanoparticle dispersion.
4. Integrating modeling of each aforementioned components into a Bayesian framework for parameter estimation.

Physical understanding will be embedded into the modeling of the intensity function and the modeling of nanoparticle characteristics and interactions. The first three parts of the strategy will be discussed in this subsection, and the Bayesian modeling framework will be discussed in Section 3.

2.1.1. *Modeling* $\mathbf{Y(s)}$ *as an inhomogeneous Poisson random field*

The concept of modeling nanoparticle dispersion using an inhomogeneous Poisson random field, which is a direct extension of a Poisson process from one dimension to two or higher dimensions, stems from the observation that the number of nanoparticles in each unit area/volume and its variability at the nanoscale represent the uniformity of nanoparticle distribution in polymer matrices. For simplicity, let us take a two-dimensional model as an example.

Suppose Fig. 2 shows a cross-section view of a nanocomposite material at a fine scale. Clearly, the number of nanoparticles/clusters in a unit area or volume varies from region to region, and it reveals the degree of uniformity of nanoparticle dispersion on the observed surface.

Therefore, modeling nanoparticle dispersion is the same as modeling the number of nanoparticles in sites $\mathbf{s} = \{1, 2, \ldots, n\}$ that are regular divisions of the nanocomposite surface/volume and have relatively small sizes. Consequently, similar to modeling event occurrences through the inhomogeneous Poisson process with a time-dependent occurrence rate, modeling $\mathbf{Y(s)}$ as an inhomogeneous Poisson random field with site-dependent intensity function $\lambda(\mathbf{s}, \boldsymbol{\beta})$ should also be appropriate to establish the dispersion model for nanoparticles.

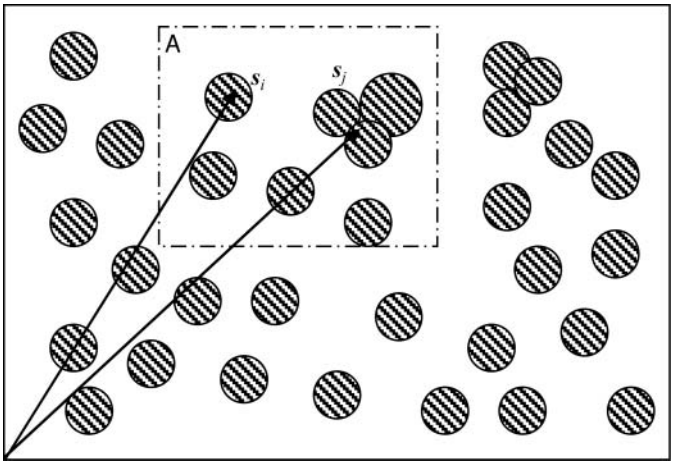

Fig. 2. Inhomogeneous Poisson random field model for particle dispersion.

2.1.2. *Intensity function modeling of the inhomogeneous Poisson random field*

Modeling of the intensity function $\lambda(\mathbf{s}, \boldsymbol{\beta})$ includes two major components. One is the linear regression part, incorporating the effects of various process variables (e.g., mixing time, temperature, and volume fraction of added nanoparticles) and the characteristics of the nanoparticles/clusters (e.g., the effective size, which refers to the diameter of a nanoparticle or the size of a cluster consisting of several nanoparticles, such as s_j shown in Fig. 2). The other part is a random field $\Psi(\mathbf{s})$ with a special covariance structure to characterize interparticle interactions.

One potential problem with this modeling strategy is that some of the process variables and nanoparticle characteristics are hard to quantify due to process uncertainties. For example, during the mixing process, small transient temperature variations may arise locally because of the heat generated from friction and the shear forces of the viscous fluid. A given volume element, such as region A in Fig. 2, may contain several particles or clusters, making it difficult to choose an effective particle size for the intensity function. Furthermore, different process variables or nanoparticle characteristics may also have mutual dependence. For instance, the effective particle sizes are affected by temperature and pH values. The regression part will become too complex if all possible interactions among process variables and nanoparticle characteristics are directly modeled as components of it. Therefore, we propose to model process variables and nanoparticle characteristics individually if necessary and adopt a hierarchical modeling structure for their integration. Detailed development of such integration will be discussed in the following sections.

2.1.3. *Intensity function as a measure for nanoparticle dispersion*

Although the intensity function is not a direct measure of the dispersion performance, it is a good index at fine scale to represent the nanoparticle dispersion state for the following reasons:

1. As the length scale goes to the nanoscale, the number of nanoparticles governed by the intensity function in each unit area represents the uniformity of nanoparticle dispersion on the whole nanocomposite.
2. The intensity model considers effective particle/cluster sizes. The size distribution across sites indicates whether there exist agglomerates or clusters.
3. Physical interaction among nanoparticles is incorporated in $\Psi(\mathbf{s})$. Deviation from the intended covariance structure could also indicate inappropriate dispersion.

Hence, we propose the intensity function as a quantitative measure of nanoparticle dispersion at the nanoscale to facilitate control and diagnosis of the nanocomposite fabrication process.

2.2. *Modeling of nanoparticle dispersion*

As discussed previously, we denote $\mathbf{Y}(\mathbf{s}) = \{Y(1), Y(2), \ldots, Y(n)\}^{\mathrm{T}}$ to be the total numbers of nanoparticles in the areas of sites $\mathbf{s} = \{1, 2, \ldots, n\}$ that are regular divisions of the polymer–nanoparticle composite surface/volume. We model $\mathbf{Y}(\mathbf{s})$ as an inhomogeneous Poisson random field with an intensity function $\lambda(\mathbf{s}, \boldsymbol{\beta})$. That is,

$$\Pr\left(Y(\mathbf{s}) = m\right) = \exp\left\{-\lambda(\mathbf{s}, \boldsymbol{\beta})\right\} \cdot \frac{\left\{\lambda(\mathbf{s}, \boldsymbol{\beta})\right\}^{m}}{m!} \qquad (2)$$

where $m = 0, 1, \ldots,$ and $s = 1, 2, \ldots, n$.

For the intensity function $\lambda(\mathbf{s}, \boldsymbol{\beta})$, if we let $\mathbf{X}$ represent the collection of the influential process variables (mixing time, temperature, density of the master batch of nano-SiO_2/epoxy, rotation speed, pH value, volume fraction of added nanoparticles, etc.) and nanoparticle characteristics (effective size of nanoparticles/clusters), $\boldsymbol{\beta}$ the corresponding unknown regression coefficients, and $\Psi(\mathbf{s})$ the random field to capture interparticle interactions, then $\lambda(\mathbf{s}, \boldsymbol{\beta})$ can be represented as

$$\lambda(\mathbf{s}, \boldsymbol{\beta}) = \exp\left\{\mathbf{X}^{\mathrm{T}}(\mathbf{s})\boldsymbol{\beta} + \Psi(\mathbf{s})\right\}. \qquad (3)$$

That is, the log of the intensity function $\lambda(\mathbf{s}, \boldsymbol{\beta})$ is a linear regression of $\mathbf{X}$ plus a correlated error term $\Psi(\mathbf{s})$, in contrast to the independent noises in ordinary linear regressions.

Due to process uncertainties, process variables or nanoparticle characteristics will be represented by probability distributions with model parameters $\boldsymbol{\xi}$ (e.g., $\mu(d)$ and $\sigma(d)$ for effective particle size: d). And for each element in $\boldsymbol{\xi}$, there may still be a probability distribution for it involving parameters $\boldsymbol{\theta}$. The configuration of these probability distributions will be correlated with physical process knowledge and will be defined only when necessary. Denote g, f to be corresponding possible distribution functions for a process or characteristic variable $X \in \mathbf{X}^T$ and a parameter in $\boldsymbol{\xi}$, then our model states:

$$X\left|\boldsymbol{\xi} \sim g\left(\boldsymbol{\xi}\right|\boldsymbol{\theta}\right), \text{and}\, \xi\left|\boldsymbol{\theta} \sim f\left(\boldsymbol{\theta}\right).\right. \qquad (4)$$

The correlated error terms $\Psi(\mathbf{s})$ will be modeled as a Gaussian Markov Random Field (GMRF), which defines the neighbors for each site and the conditional distribution of $\Psi(\mathbf{s})$ given the values of its neighboring sites to capture the hard-to-model interaction force field among nanoparticles. The mathematical form of a GMRF is represented as follows:

$$\Psi(s)|\Psi(s'), s' \neq s \sim N(\mu, \sigma^2(s)), \qquad (5)$$

where $s, s' \in \{1, 2, \ldots, n\}$, $\mu = \sum b(s, s'')\Psi(s''), s'' \in$ {neighbors of s} and $\sigma^2(s)$ is the unknown conditional variance of $\Psi(\mathbf{s})$. Equation (5) states that the conditional distribution for each $\Psi(\mathbf{s})$ is a normal distribution with parameters only related to its neighboring sites.

One advantage of modeling using a GMRF is that the GMRF provides a unified modeling representation for diverse correlation structures. This property is especially important in our case, where there is limited knowledge about the correlation structure and hence no parametric covariance functions can be derived. Besides, there are fast and efficient algorithms for transforming between GMRF and commonly used covariance functions and force fields. Hence, we can easily integrate GMRF with existing and forthcoming physical knowledge. For example, we can link it with the commonly used Lennard–Jones (L–J) potential functions (Zeng *et al.*, 2008) to characterize the interaction potential among nanoparticles. By performing the transformation between the L–J potential and GMRF, not only can we make use of prior knowledge of the L–J potential to get a better initial setting but we can also gain more understanding of the process–interaction relations when statistical estimation from real collected data is obtained. Examples of linking GMRF with the L–J potential function will be demonstrated in Section 4 during the case studies.

3. Bayesian hierarchical framework for parameter estimation

Based on our modeling strategies presented in Section 2.1, we integrate the models specified by Equations (1) to (5) into a Bayesian hierarchical modeling framework for parameter estimation. Figure 3 depicts the framework, together with its comparison to classical hierarchical models (Rubin, 1980). We borrow the graphical representation from Huang (2011).

Three sources of data, namely, process data, product data, and prior physical knowledge for hyper-parameters $\boldsymbol{\theta}$, constitute the model inputs. The process data may include process parameters that can be quantified such as

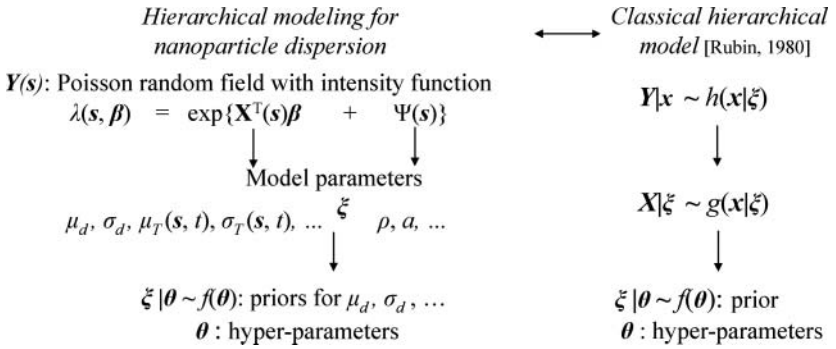

Fig. 3. Bayesian hierarchical modeling framework (after Huang (2011)).

the pH value, volume fraction of added nanoparticles, etc. Product data comprise the number of nanoparticles in each site counted from SEM or TEM images. Prior physical knowledge for the hyper-parameters θ will be used to set initial distributions.

There are two major advantages of adopting the Bayesian hierarchical framework:

1. Offline SEM or TEM inspection is extremely time-consuming and only provides information on a very tiny surface area of the nanocomposite. The Bayesian hierarchical framework can effectively estimate a large number of parameters with limited data.
2. Normally no analytical solution exists for the hierarchical model specified through Equations (1) to (5). While traditional maximum likelihood estimation is hard to implement here, the Bayesian hierarchical structure allows us to use Markov Chain Monte Carlo (MCMC) simulation to obtain the model parameter estimation.

Given process and product data and prior distributions for hyper-parameters θ, conditional distributions of θ under available settings can be obtained. By sequentially drawing samples via the MCMC method, we could ultimately estimate θ, ξ, and β in the model (Fig. 3). Consequently, the process–dispersion relations can be estimated based on real collected data. Dispersion of nanoparticles can thus be predicted under various process conditions. Finer degrees of control of nanocomposite properties will become possible based on the proposed quantitative modeling of nanoparticle dispersion.

4. Case studies

Case studies are conducted to illustrate the proposed nanoparticle dispersion modeling approach. First, a simulation study is used to demonstrate the modeling procedure and validate the parameter estimation algorithm. Then, real experimental data will be analyzed to characterize the nanoparticle dispersion under different process conditions. The MCMC is performed using WinBUGs software in this article.

In both studies, the following procedures are followed:

1. Two nanoparticle dispersion images are obtained with different parameter settings of a manufacturing process through the simulation or the real fabrication processes.
2. The images analyzed in the simulation study are divided into 225 grids and the ones obtained from real fabrication are divided into 196 grids due to the image size of collected samples.
3. Model parameter estimation and nanoparticle dispersion prediction are obtained using the MCMC technique with WinBUGs.
4. Evaluation and discussion of obtained results are provided in both case studies.

4.1. *Simulation study and discussion*

The simulation dataset was designed to mimic the nanoparticle dispersion images taken from the nanocomposite specimen manufactured under different mixing processes. We assumed that the nanoparticle dispersion followed an inhomogeneous Poisson random field with intensity function as defined in Equations (2) to (4) of Section 2. We also assumed that the nanoparticle interaction follows a modified L–J potential listed below:

$$V(r) = 4\rho \left\{ \left(\frac{a}{r + r_0} \right)^6 - \left(\frac{a}{r + r_0} \right)^{12} \right\}. \qquad (6)$$

In Equation (6), r stands for the distance between any two different sites on the same image and $r_0^6 = 2(\rho + \sqrt{\rho^2 - 1}) \times |a|^6$ so that $V(0) = 1$. The parameters used in the simulation included the volume fraction of nanofillers (a process variable); effective size of the nanoparticles/clusters, which was assumed to follow a normal distribution for both images; and regression coefficients (β_0 as the ground intercept, β_1 as the coefficient for volume fraction, and β_2 as the coefficient for effective particle/cluster size). Please refer to Table 1 for a summary of specified parameter values. The simulated images are presented as Figs. 4(a) and 4(b).

Table 1. Summary of specified β and ξ for dataset generation in the simulation study

	Regression coefficients (β)			*Model parameters (ξ)*				
				Volume fraction	*Nanoparticle effective size*		*Modified L–J potential*	
	β_0	β_1	β_2	v	$\mu_d\,(nm)$	$\sigma_d^2\,(nm^2)$	ρ	a
Specified selections	2.10	1.60	0.07	(0.02, 0.15)	25	4	2.50	1.50

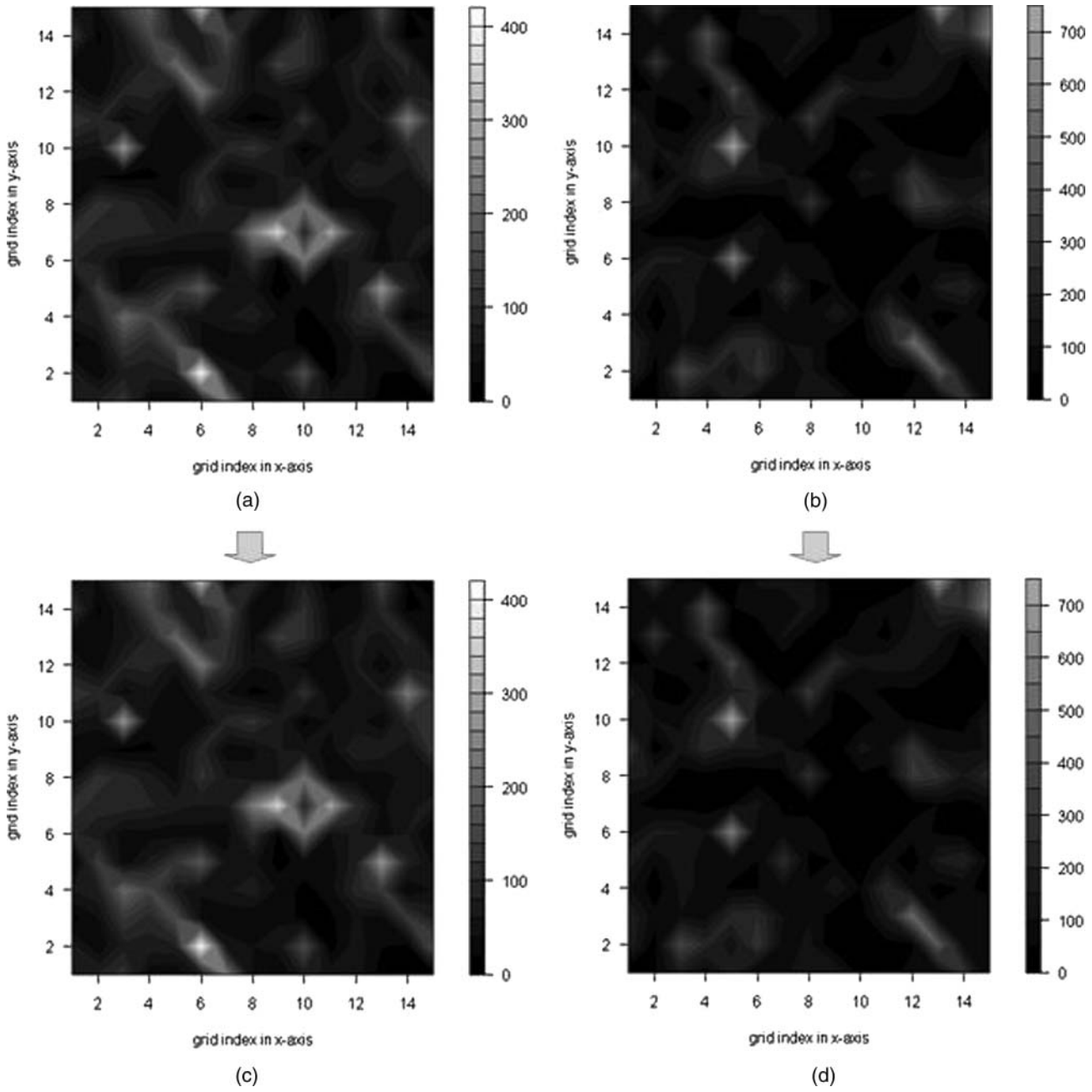

Fig. 4. Comparison of the number of nanoparticles dispersed in the simulated and predicted samples: (a) simulated image with 2 vol.% and (b) simulated image with 15 vol.%, (c) predicted image with 2 vol.%, and (d) predicted image with 15 vol.% nanoparticles introduced.

Table 2. Bayesian estimates via MCMC for simulation data study

Parameter	*Mean*	*Std. dev.*	*Median*	*95% C.I.*
β_0	1.097	0.954	0.665	[0.025, 3.231]
β_1	1.772	0.197	1.774	[1.374, 2.160]
β_2	0.1116	0.038	0.129	[0.026, 0.155]
ρ	2.180			
a	1.184			

As mentioned before, we followed the modeling procedures in Section 2 and re-estimated these model parameters using the MCMC technique in WinBUGs. The non-informative priors of regression coefficients ($\boldsymbol{\beta}$) were set as β_0, β_1, and $\beta_2 \sim$ uniform(0, 50) in this hierarchical model. In addition, we ran three Markov chains simultaneously with different initial values that were far apart from each other. The first 30 000 runs were truncated to reduce the parameter estimation inaccuracy, which is the so-called burn-in process, and the following 90 000 iterations were used to compute posterior statistics of the investigated parameters. The obtained parameter estimations are summarized in Table 2, where "95% C.I." refers to the 95% confidence interval (e.g., Type I error equals to 5%).

Based on Table 2, it is clear that the estimated confidence intervals for regression coefficients ($\boldsymbol{\beta}$) cover the designated values in Table 1. Moreover, we modeled the nanoparticle interaction as first-order CAR model and re-estimated ρ and a in the modified L–J potential. The estimation results of the regression coefficients and the L–J potential parameters support the effectiveness of the proposed estimation algorithm. Table 2 also shows that if the volume fraction of the nanoparticles is high, the estimated mean value of the intensity function is high, which matches our intuition.

The four panels of Fig. 4 are used to compare the number of dispersed nanoparticles from the generated simulation data-set with the ones obtained by the model predictions. In each panel, the image plot shows the number of dispersed nanoparticles associated with each grid, s, and the x- and y-axes are the indices for different grids. To be more specific, Figs. 4(a) and 4(b) are the number of nanoparticles counted from simulated specimens and the predicted numbers of nanoparticles for these two specimens are plotted as Figs. 4(c) and 4(d), which are actually equal to the estimated values of the intensity function. The left column in Fig. 4 is for a nanocomposite with 2 vol.% nanoparticles and the right column is a nanocomposite with 15 vol.% nanoparticles. Overall, it is clear that the patterns of the nanoparticle dispersion look quite similar in the plots of the simulated and the prediction data.

4.2. *Real image data study and discussion*

Figures 5(a) and 5(b) show two images taken from real nanocomposite surfaces after the mixing process and the size of each photo is about 700×700 nm^2. Each of them is further divided into 196 sites in total, which is determined by the appropriate cross-section size suggested by the domain experts. We used these two images to develop the quantitative model for nanoparticle dispersion characterization.

Based on domain experts' knowledge, the influential process variables are similar to the ones we used in the simulation case study including volume fraction, v, and effective particle/cluster size, d. Since the temperature was maintained at the same degree throughout the whole mixing process, it was eliminated from the analysis.

The hierarchical modeling structure and the parameter estimation process were carried out similarly to what was done in the simulation study. The non-informative priors

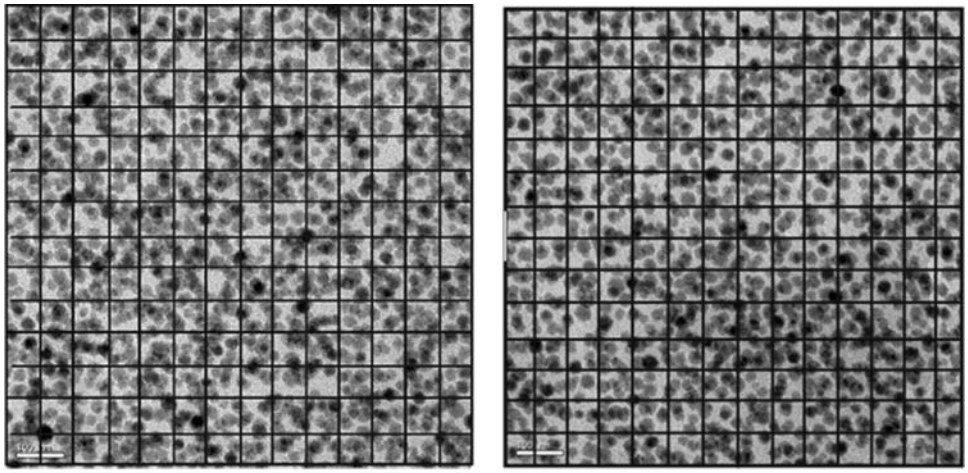

Fig. 5. Two TEM images with grid line taken from the silica/epoxy nanocomposites with different amount of nanoparticles introduced: (a) 9 vol.% and (b) 14 vol.%.

Table 3. Bayesian estimates via MCMC for real experimental images (silica/epoxy nanocomposite with 9 vol.% and 14 vol.% induced nanoparticles)

Parameter	*Mean*	*Std. dev.*	*Median*	*95% C.I.*
β_0	0.929	0.577	0.862	[0.064, 2.173]
β_1	4.399	1.156	4.395	[2.135, 6.679]
β_2	−0.011	0.023	−0.009	[−0.060, 0.025]
ρ	2.800			
a	2.285			

of regression coefficients ($\boldsymbol{\beta}$) were set as $\beta_0 \sim$ uniform(0, 10), $\beta_1 \sim$ normal(0, $1e^5$) and $\beta_2 \sim$ normal(0, $1e^5$) in the hierarchical model. Similarly, we adopted the first-order CAR model in this analysis to model the nanoparticle interactions.

Table 3 summarizes the parameter estimation results obtained from the three different Markov chains after the burn-in process. Here the regression coefficients are consistent with the notations defined earlier in the simulation study. Based on the estimated regression coefficients

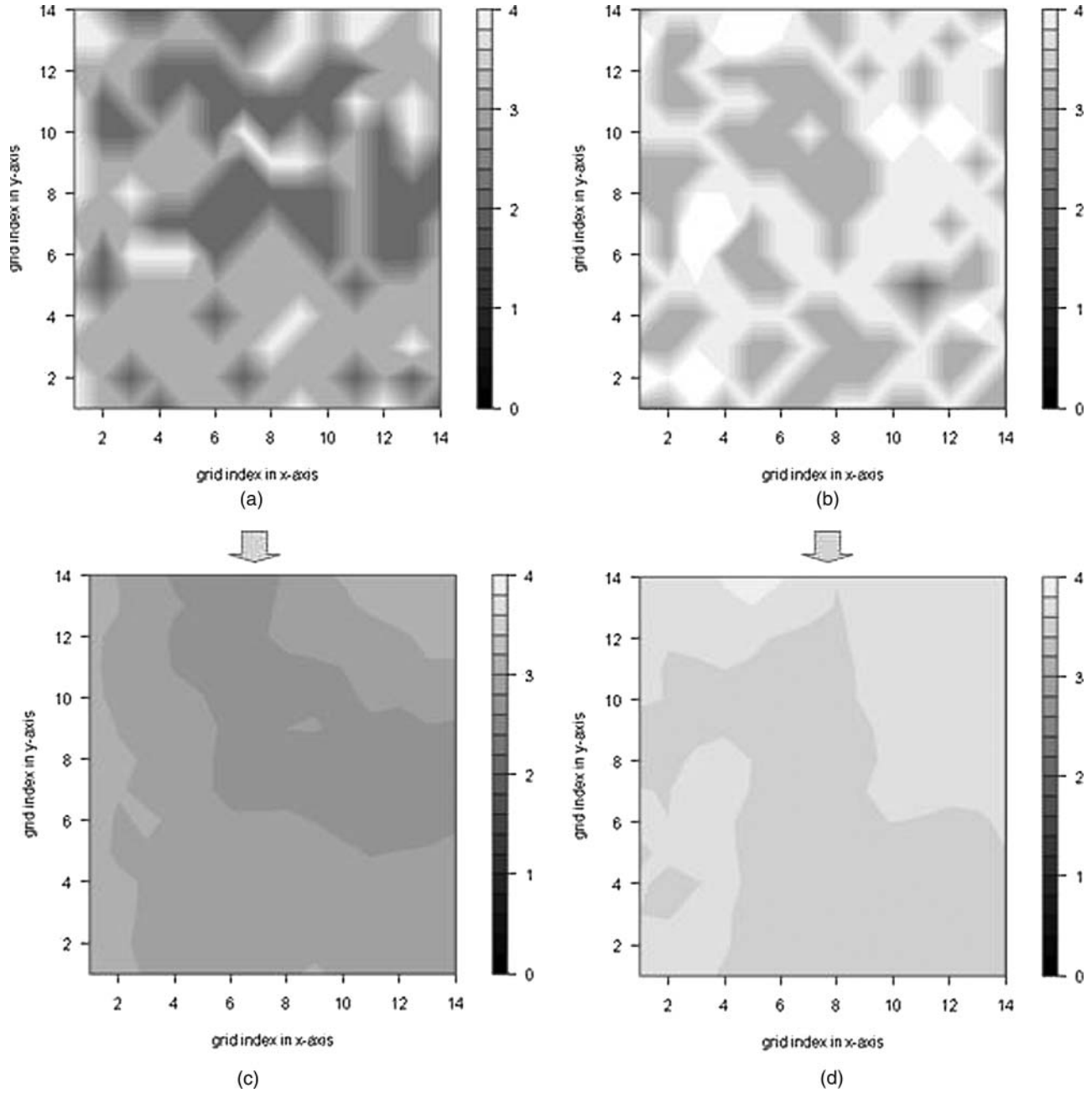

Fig. 6. Comparison of counted nanoparticle dispersion states between true image and model prediction: (a) true image with 9 vol.%, (b) true image with 14 vol.%, (c) prediction with 9 vol.%, and (d) prediction with 14 vol.% silica/epoxy nanocomposites.

in Table 3, it is clear that increasing the volume fraction of nanofillers will increase the density of dispersed nanoparticles. Also, the site with a larger effective nanoparticle/cluster size will tend to have fewer nanoparticles dispersed.

To clearly represent the counting quantity **Y(s)** at a fine scale, Figs. 6(a) and 6(b) plot the counted number of nanoparticles dispersed at each site on the two nanocomposite images; Figs. 6(c) and 6(d) are the predicted number of dispersed nanoparticle through WinBUGs. Note that images on the left in Fig. 6 are the images for 9 vol.% silica/epoxy nanocomposites and the images on the right are those for 14 vol.% silica/epoxy. The predictions are the estimated values of the intensity functions.

One thing that should be noted is that since we adopt the inhomogeneous Poisson random field as the key component of characterization model, the prediction actually represents the "expected" nanoparticle dispersion states in a general probabilistic realization point of view. Moreover, one interesting observation is that the 95% confidence intervals of the intensity function cover the truly counted numbers of nanoparticles in most cases, as shown in Fig. 7. The solid black dots stand for the counted numbers from

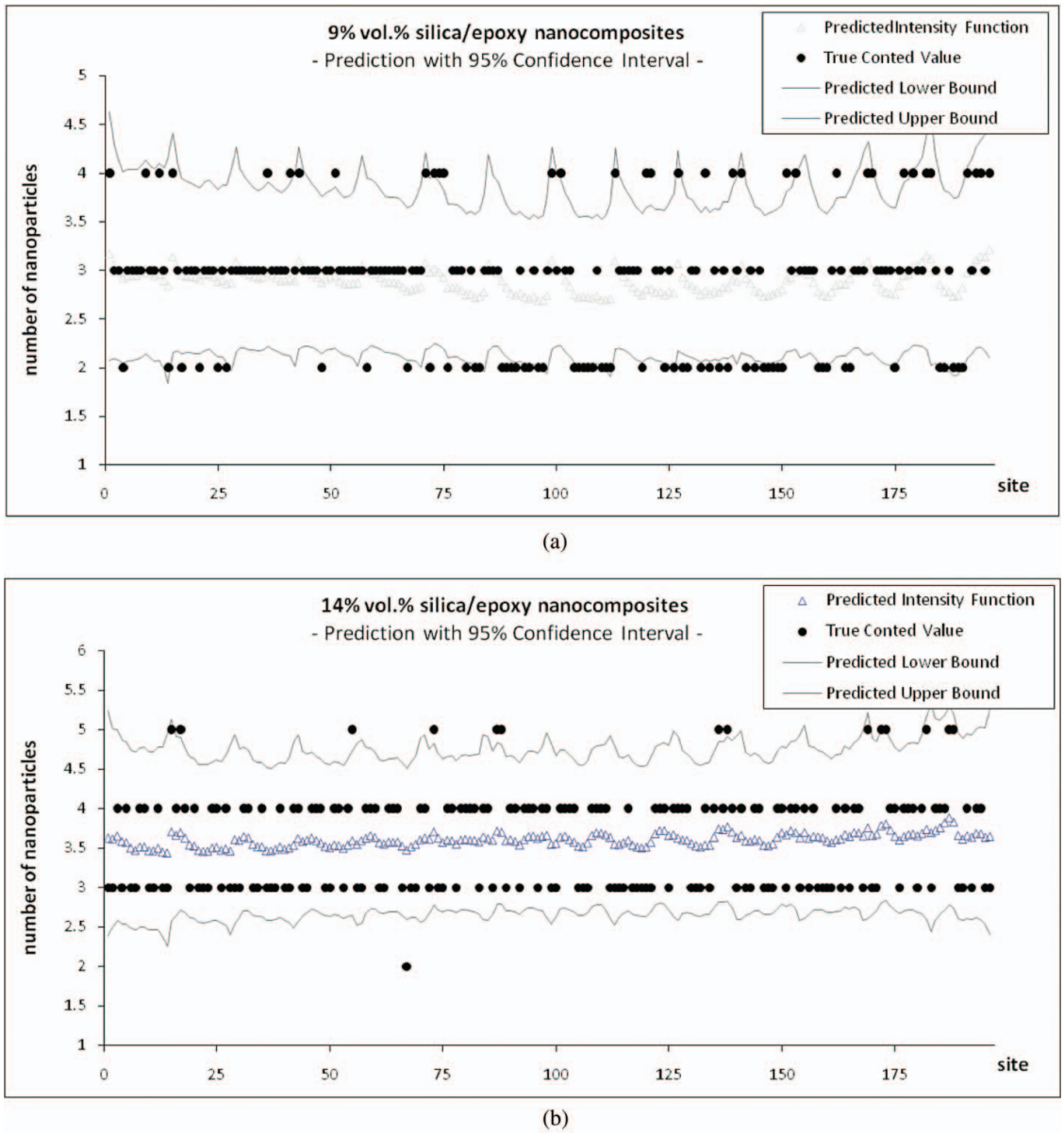

Fig. 7. Comparison of observation and prediction of nanoparticle dispersion states for (a) 9 vol.% and (b) 14 vol.% silica/epoxy nanocomposites (color figure provided online).

Table 4. Predictive ability of the proposed model

Vol. % of nanofillers for different images	*Mean of λ prediction*	*Mean of std. dev. of λ prediction*	*Mean of 95% C.I. of λ*	*Mean of truly counted numbers*
9	2.891	0.448	[2.107, 3.861]	2.883
14	3.597	0.540	[2.648, 4.764]	3.602

the real image data, while the empty triangles are the predictions whose 95% confidence bounds are depicted by gray lines in Fig. 7.

Other than looking at Fig. 7 to learn the model prediction performance, we also calculated (i) the mean of estimated intensity functions among all sites in the same image; (ii) the mean of the standard deviations of intensity functions among all sites in the same image; (iii) the mean of the 95% confidence intervals of the intensity function among all sites in the same image; and (iv) the mean of the counted number of nanoparticles among all sites in the same image, see Table 4. It is clear that the mean of the true observed number of dispersed nanoparticles counted from each TEM image is within the mean of the 95% confidence intervals of $\boldsymbol{\lambda}$. This gives another example to support the effectiveness of our proposed model structure and parameter estimation strategy.

5. Summary

Nanoparticle dispersion plays a crucial role in determining the mechanical properties of polymer nanocomposites. In this work we develop a quantitative measure to effectively describe nanoparticle dispersion based on data measured using SEM or TEM. The nanoparticle dispersion is characterized by the intensity function of an inhomogeneous Poisson random field. The intensity function is a mixture of the linear regression model and the GMRF. To be more specific, the linear regression model is constructed with process variables and nanoparticle characteristics while the GMRF is approximated from engineering knowledge of the particle interaction force. Unlike conventional modeling methods that usually rely only on pure physical laws or statistical data-driven techniques; the proposed model integrates both nanomanufacturing domain knowledge and statistical data analysis to provide a better characterization of nanoparticle dispersion states. Both simulation and experimental data analysis show the effectiveness of the proposed method.

Since the proposed model links process variables with final nanocomposite structure properties, it provides a basis for process monitoring, root cause diagnosis, and active process control; it thus deserves further investigation in the future.

Acknowledgements

Huang's work is partially supported by NSF grant CMMI-1002580. Dr. Zhong Zhang at the National Center for Nanoscience and Technology, China, provided measurement data and process knowledge regarding polymer nanocomposites.

References

Balazs, A.C., Emrick, T. and Russell, T.P. (2006) Nanoparticle polymer composites: where two small worlds meet. *Science* **314**, 1107–1110.

Chapman, R. and Mulvaney, P. (2001) Electro-optical shifts in silver nanoparticle films. *Chemical Physics Letters*, **349**, 358–362.

Hench, L.L. and West, J.K. (1990) The sol-gel process. *Chemical Reviews*, **90**, 33–72.

Huang, Q. (2011) Physics-driven bayesian hierarchical modeling of nanowire growth process at each scale. *IIE Transactions*, **43**, 1–11.

Huang, Q., Wang, L., Dasgupta, T., Zhu, L., Sekhar, P.K., Bhansali, S. and An, Y., (2011) Statistical weight kinetics modeling for silica nanowires growth catalyzed by Pd thin film. *IEEE Transactions on Automation Science and Engineering*, **8**, 303–310.

Kojima, Y., Usuki, A., Kawasumi, M., Fukushima, Y., Okada, A., Kurauchi, T. and Kamigaito, O. (1993) Mechanical properties of nylon 6-clay hybrid. *Journal of Materials Research*, **8**, 1185–1189.

Krishnamoorti, R. and Vaia, R.A. (2002) *Polymer Nanocomposites*, ACS, Washington, DC.

Mackay, M.E. Tuteja, A., Duxbury, P.M., Hawker, C.J., Van Horn, B., Guan, Z., Chen, G. and Krishnan, R.S. (2006) General strategies for nanoparticle dispersion. *Science*, **311**, 1740–1743.

Maskara, A. and Smith, D.M. (1997) Agglomeration during the drying of fine silica powders. . . . The role of particle solubility. *Journal of the American Ceramic Society*, **80**(7), 1715–1722.

Matejka, L., Dusek, K. and Noga, J. (1998) Formation, structure and mechanical properties of organic–silica hybrid networks. *Wiley Polymer Networks Group Reviews Series*, **1**, 301–311.

Rubin, D.B. (1980) Using empirical Bayes techniques in the law school validity studies. *Journal of the American Statistical Association*, **75**, 801–816.

Usuki, A., Kawasumi, M., Kojima, Y., Fukushima, Y., Okada, A., Kurauchi, T. and Kamigaito, O. (1993) Synthesis of nylon 6-clay hybrid. *Journal of Materials Research*, **8**, 1179–1184.

Weng, W.H., Chen, H., Tsai, S.P. and Wu, J.C. (2004) Thermal property of epoxy/SiO_2 hybrid material synthesized by the sol–gel process. *Journal of Applied Polymer Science*, **91**(1), 532–537.

Wilson, O., Wilson, G.J. and Mulvaney, P. (2002) Laser writing in polarized silver nanorod films. *Advanced Materials*, **14**, 1000–1004.

Yoon, P.J., Fornes, T.D. and Paul, D.R. (2002) Thermal expansion behavior of nylon 6 nanocomposites. *Polymer*, **43**, 6727–6741.

Zeng, Q.H., Yu, A.B. and Lu, G.Q. (2008) Multiscale modeling and simulation of polymer nanocomposites. *Progress in Polymer Science*, **33**, 191–269.

Zhang, H., Zhang, Z., Friedrich, K. and Eger, C. (2006) Property improvements of in situ epoxy nanocomposites with reduced interparticle distance at high nanosilica content. *Acta Materialia*, **54**, 1833–1842.

Appendix

Table A.1. The counted number of nanoparticles dispersed at each site for 9 vol.% and 14 vol.% silica/epoxy nanocomposites

		Number of nanoparticles counted at each site (*s*)																												
		1	2	3	4	5	6	7	8	9	10	11	12	13	14		1	2	3	4	5	6	7	8	9	10	11	12	13	14
9%	1	4	4	3	4	3	4	3	4	4	4	4	3	4	4	14%	1	3	5	3	4	3	4	4	3	3	4	4	4	5	3
	2	3	3	3	3	2	2	3	3	3	2	2	3	4	3		2	3	4	3	3	4	3	3	3	3	4	3	3	3	4
	3	3	2	3	3	3	4	3	4	3	2	3	3	3	2		3	4	5	4	3	4	5	5	4	3	4	3	4	3	4
	4	2	3	3	3	3	4	2	3	3	3	2	2	3	2		4	3	4	4	4	4	3	5	4	4	3	4	3	5	4
	5	3	3	3	3	3	4	2	3	3	3	3	2	3	3		5	4	3	3	4	3	3	3	4	3	3	4	3	5	5
	6	3	3	3	2	3	2	2	2	3	2	2	2	3	2		6	3	4	3	4	3	4	4	4	3	3	3	3	4	5
	7	3	2	3	3	3	3	2	2	2	4	2	3	2	2		7	3	3	4	3	4	4	4	3	3	4	3	3	4	3
	8	3	3	4	3	3	3	3	2	4	2	2	4	3	2		8	4	3	3	3	4	3	3	3	3	3	3	4	3	3
	9	4	3	3	4	3	3	2	2	4	3	2	3	4	4		9	4	3	3	4	4	4	4	3	3	4	4	3	4	4
	10	3	3	3	3	3	2	2	2	3	2	2	2	3	3		10	3	4	3	4	3	4	4	4	4	5	4	4	4	3
	11	3	2	3	3	2	3	3	3	3	3	4	2	4	4		11	3	4	4	3	2	4	4	4	4	4	3	3	4	4
	12	4	3	3	3	3	2	2	2	2	2	3	3	3	4		12	4	3	3	4	3	4	3	4	4	5	4	4	3	4
	13	3	2	4	3	3	2	2	2	3	4	4	3	3	3		13	3	4	3	5	3	3	4	4	3	4	4	4	4	3
	14	2	3	3	3	3	3	3	2	2	3	3	3	4	4		14	3	3	4	3	4	4	4	3	4	3	3	3	5	3

Biographies

Chia-Jung Chang is a Ph.D. student in the H. Milton Stewart School of Industrial and Systems Engineering at the Georgia Institute of Technology. She received both her B.S. and M.S. degrees in the Industrial Engineering and Engineering Management Department at National Tsing-Hua University in Taiwan in 2005 and 2007, respectively. She will join the Harold and Inge Marcus Department of Industrial and Manufacturing Engineering at Pennsylvania State University in 2012. Her research interests focus on quality engineering and applied statistics, system informatics and control of complex systems, and design of experiments. She is a member of ASA, IIE, and INFORMS.

Lijuan Xu is a Ph.D. student in the Daniel J. Epstein Department of Industrial and Systems Engineering at the University of Southern California, Los Angeles. She received her B.S. degree from the Department of Industrial and Systems Engineering of Tsinghua University, China, in 2009. She is currently pursuing a Ph.D. degree in the Daniel J. Epstein Department of Industrial and Systems Engineering at the University of Southern California, Los Angeles, California. Her research focuses on modeling of and estimation of nanostructure spatial interactions for nanomanufacturing quality control.

Qiang Huang is currently an Associate Professor and Gordon S. Marshall Early Career Chair in Engineering in the Daniel J. Epstein Department of Industrial and Systems Engineering at the University of Southern California, Los Angeles. He was previously an Assistant Professor and then an Associate Professor in the Department of Industrial and Management Systems Engineering at the University of South Florida from 2003 to 2009. Funded by the National Science Foundation (including CAREER award) and ONR, his research focuses on modeling and analysis of complex systems for quality and productivity improvement, with special interest in integrated nanomanufacturing and nanoinformatics. He is an Associate Editor of *IEEE Transactions on Automation Science and Engineering* since 2012 and served as Editor (Quality, Micro and Nanomanufacturing Systems) for the *Journal of Manufacturing Systems* from 2008 to 2011. He was one of the editors for the special issue of the *IIE Transactions*: "Quality, Sensing and Prognostics Issues in Nanomanufacturing." He was a member of the scientific committee (Editorial Board) for the North American Manufacturing Research Institution (NAMRI) of SME, 2009–2011. He was an Associate Editor (Automation in Meso, Micro and Nano-Scale) of the 2009 and 2010 IEEE Conferences on Automation Science and Engineering. He is a member of IIE, INFORMS, IEEE, SME, and ASME.

Jianjun Shi is Carolyn J. Stewart Chair Professor at the H. Milton Stewart School of Industrial and Systems Engineering, Georgia Institute of Technology. Before joining Georgia Tech in 2008, he was the G. Lawton and Louise G. Johnson Professor of Engineering at the University of Michigan. He was awarded his B.S. and M.S. in Electrical Engineering by the Beijing Institute of Technology in 1984 and 1987, respectively, and his Ph.D. in Mechanical Engineering at the University of Michigan in 1992. His research interests focus on the fusion of advanced statistics, signal processing, control theory, and domain knowledge to develop methodologies for modeling, monitoring, diagnosis, and control for complex systems in a data-rich environment. He was the founding chairperson of the Quality, Statistics and Reliability (QSR) Subdivision at INFORMS. He currently serves as a Focus Issue Editor for *IIE Transactions*. He is a Fellow of the Institute of Industrial Engineering, a Fellow of the American Society of Mechanical Engineering, a Fellow of the Institute of Operations Research and Management Science, and a life member of ASA.